

This discussion paper is/has been under review for the journal Biogeosciences (BG).  
Please refer to the corresponding final paper in BG if available.

# Environmental controls on the greening of terrestrial vegetation across northern Eurasia

P. Dass<sup>1</sup>, M. A. Rawlins<sup>1</sup>, J. S. Kimball<sup>2</sup>, and Y. Kim<sup>3</sup>

<sup>1</sup>Climate System Research Center, Department of Geosciences, University of Massachusetts, Amherst, MA, USA

<sup>2</sup>FLBS/NTSG, Univ. of Montana, Missoula, MT, USA

<sup>3</sup>NTSG, College of Forestry and Conservation, University of Montana, Missoula, MT, USA

Received: 28 May 2015 – Accepted: 29 May 2015 – Published: 18 June 2015

Correspondence to: P. Dass (pawlok.dass@gmail.com)

Published by Copernicus Publications on behalf of the European Geosciences Union.

**BGD**

12, 9121–9162, 2015

## Vegetation greening across northern Eurasia

P. Dass et al.

Title Page

Abstract

Introduction

Conclusions

References

Tables

Figures



Back

Close

Full Screen / Esc

Printer-friendly Version

Interactive Discussion



## Abstract

Terrestrial ecosystems of northern Eurasia are greening, yet few studies have provided definitive attribution for the changes. While prior studies point to increasing temperatures as the principle environmental control, influences from moisture and other factors are less clear. We assess how changes in temperature, precipitation, cloudiness and forest fires contribute to the trend in Gross Primary Productivity (GPP) derived from satellite data across northern Eurasia. For the period 1982–2008 we find that GPP, estimated using ensemble satellite NDVI (Normalized Difference Vegetation Index) observations from GIMMS3g and VIP datasets, is most sensitive to temperature, precipitation and cloudiness during summer, the peak of the growing season. For regional median GPP, summer temperature explains 33.3% of the variation in GPP, while the other environmental variables explain from 2.2 to 11.8%. Warming over the period analyzed, even without a sustained increase in precipitation, led to a significant GPP increase over 67.3% of the region. A significant decrease in GPP was found over 6.2% of the region, primarily the dryer grasslands in the south-western. For this area, precipitation positively correlates with GPP, as does cloudiness. This shows that the south-western part of northern Eurasia is relatively more vulnerable to drought than other areas. Our results further advance the notion that air temperature is the dominant environmental control for the recent GPP increases across northern Eurasia.

## 1 Introduction

Several analyses of Normalized Difference Vegetation Indices (NDVI) data derived from satellite remote sensing have pointed to greening, i.e. a positive trend in Gross Primary Productivity (GPP) and Leaf Area Index (LAI) of the northern high latitudes in the recent decades (Myneni et al., 1997; Carlson and Ripley, 1997; Zhou et al., 2001; Guay et al., 2014). Warming has also occurred over this time. Global mean surface air temperatures increased by 0.2 to 0.3°C over the past 40 years with warming greatest

**BGD**

12, 9121–9162, 2015

## Vegetation greening across northern Eurasia

P. Dass et al.

Title Page

Abstract

Introduction

Conclusions

References

Tables

Figures



Back

Close

Full Screen / Esc

Printer-friendly Version

Interactive Discussion



across northern land areas around 40–70° N (Nicholls et al., 1996; Overpeck et al., 1997). Precipitation increases have also been observed over both North America and Eurasia over the past century (Nicholls et al., 1996; Groisman et al., 1991). Urban et al. (2014) describe the co-occurrence of these climatic and ecosystem changes.

Here we investigate greening of terrestrial ecosystems of northern Eurasia and determine the relative attribution arising through changes in several geophysical quantities, hereinafter referred to as “environmental variables”, as they potentially drive observed temporal changes in vegetation productivity.

Gross Primary Productivity (GPP) is a physical measure of the rate of photosynthesis, or the rate at which atmospheric CO<sub>2</sub> is fixed by autotrophic (generally green) plants to form carbohydrate molecules. Photosynthesis, being a biological process, is regulated by several environmental factors. Productivity is highest at the optimum temperature, though this optimum can be modified by cold or warm acclimation (Larcher, 1969, 2003). Water availability also affects plant hydraulics and chemistry by controlling the nutrient uptake through shoot transportation (Sharp et al., 2004; Stevens et al., 2004). Increasing atmospheric CO<sub>2</sub> concentration increases GPP by biochemical fertilization for C<sub>3</sub> plants and increasing water use efficiency for both C<sub>3</sub> and C<sub>4</sub> plants (Bowes, 1996; Rötter and Geijn, 1999).

There is both direct and indirect evidence of increasing productivity across the northern high latitudes. Flask and aircraft-based measurements show that the seasonal amplitude of atmospheric CO<sub>2</sub> concentration across the Northern Hemisphere has increased since the 1950s, with the greatest increases occurring across the higher latitudes (Graven et al., 2013). This trend suggests a considerable role of northern boreal forests, consistent with the notion that warmer temperatures have promoted enhanced plant productivity during summer and respiration during winter (Graven et al., 2013; Kim et al., 2014; Myneni et al., 1997). Observed at eddy covariance sites, Net Ecosystem Exchange (NEE), the inverse of Net Ecosystem Productivity (NEP), is a strong function of mean annual temperature at mid and high latitudes, up to the optimum temperature of approximately 16 °C, above which moisture availability overrides the tem-

## BGD

12, 9121–9162, 2015

### Vegetation greening across northern Eurasia

P. Dass et al.

Title Page

Abstract

Introduction

Conclusions

References

Tables

Figures



Back

Close

Full Screen / Esc

Printer-friendly Version

Interactive Discussion



perature influence (Yi et al., 2010). Highlighting the importance of precipitation, other studies have found vulnerabilities in ecosystems of North America as well as Eurasia from warming-related changes in hydrological patterns (Parida and Buermann, 2014; Buermann et al., 2014). With warming, low temperature constraints to productivity have relaxed (Nemani et al., 2003; Zhang et al., 2008; Yi et al., 2013). Tree-ring data suggest that black spruce forests have experienced drought stress during extreme warmth (Walker et al., 2015). Over northern Eurasia, precipitation trends have complicated the relationship between temperature and productivity, as the increasing moisture constraints have made northern Eurasia more drought sensitive (Zhang et al., 2008; Yi et al., 2013). Increasing atmospheric CO<sub>2</sub> concentration is another factor, as CO<sub>2</sub> fertilization has been demonstrated through observations, models, and FACE (Free-Air CO<sub>2</sub> Enrichment) experiments (Ainsworth and Long, 2005; Hickler et al., 2008; Graven et al., 2013). Cloudiness or shade can strongly influence vegetation productivity (Roderick et al., 2001), particularly over northern Eurasia (Nemani et al., 2003). Disturbances through forest fires also affect vegetation productivity by destroying existing vegetation and allowing for regeneration (Goetz et al., 2005; Amiro et al., 2000; Reich et al., 2001).

The role of temperature and precipitation in the greening of northern high latitudes, especially northern Eurasia has not been firmly established. Few studies have examined the effect of CO<sub>2</sub> concentration, cloudiness and forest fires. Of these environmental variables, CO<sub>2</sub> concentration is unlike the others, given its long atmospheric lifetime (~ 100–300 years) (Blasing, 2009). Thus, CO<sub>2</sub> concentration is assumed to be more spatially uniform. As a result, any statistical analysis using this variable will not be comparable with the other variables. Thus we do not analyze the influence of CO<sub>2</sub> concentration. While some studies have focused on terrestrial ecosystems of the pan-Arctic (Urban et al., 2014; Myneni et al., 1997; Guay et al., 2014; Kim et al., 2014) or the high latitudes of North America (Goetz et al., 2005; Buermann et al., 2013; Thompson et al., 2006), few studies have investigated the relative role of different environmental variables on greening of northern Eurasia. Therefore, we assess in this study how

## Vegetation greening across northern Eurasia

P. Dass et al.

Title Page

Abstract

Introduction

Conclusions

References

Tables

Figures



Back

Close

Full Screen / Esc

Printer-friendly Version

Interactive Discussion



vegetation trends in northern Eurasia are influenced by the environmental variables air temperature, precipitation, cloudiness and forest fire. Objectives are to (1) calculate the long term trend of both GPP and the environmental variables; (2) assess the magnitude of the effect of the variables on GPP; (3) identify the seasonality of the variables; (4) identify the regions of northern Eurasia where the variables boost or reduce GPP. Exploiting the availability of long term time series data we perform a spatially explicit grid point statistical analysis to achieve the above objectives.

## 2 Data and methods

### 2.1 Data

#### 2.1.1 Land cover

The study domain is the Northern Eurasia Earth Science Partnership Initiative (NEESPI) region (Groisman and Bartalev, 2007), defined as the area between 15° E longitude in the west, the Pacific coast in the east, 45° N latitude in the south and the Arctic Ocean coast in the north. Total area of this region is 22.4 million km<sup>2</sup>. Land cover distribution for the region is drawn from the Moderate Resolution Imaging Spectroradiometer (MODIS) MCD12Q1 Land Cover Product Type 5 Land Cover Product for the year 2007, available online at [https://lpdaac.usgs.gov/data\\_access/data\\_pool](https://lpdaac.usgs.gov/data_access/data_pool) from Land Processes Distributed Active Archive Center (LP DAAC), Sioux Falls, South Dakota, USA The product provides global land cover at 1 km spatial resolution, produced from several classification systems, principally that of the International Geosphere-Biosphere Program (IGBP). Friedl et al. (2002) describe the supervised classification methodology which leveraged a global database of training sites interpreted from high-resolution imagery. The GPP products used in this study (described below) use a static land cover (LC) classification to define biome response characteristics over the study record. Thus the effect of each environmental variable accounts only

**BGD**

12, 9121–9162, 2015

## Vegetation greening across northern Eurasia

P. Dass et al.

Title Page

Abstract

Introduction

Conclusions

References

Tables

Figures



Back

Close

Full Screen / Esc

Printer-friendly Version

Interactive Discussion



**BGD**

12, 9121–9162, 2015

**Vegetation greening  
across northern  
Eurasia**

P. Dass et al.

[Title Page](#)[Abstract](#)[Introduction](#)[Conclusions](#)[References](#)[Tables](#)[Figures](#)[⏪](#)[⏩](#)[◀](#)[▶](#)[Back](#)[Close](#)[Full Screen / Esc](#)[Printer-friendly Version](#)[Interactive Discussion](#)

for changes in NDVI and does not track potential changes in land cover type. While the GPP products use the standard IGBP MODIS global land cover classification, for our statistical analysis we simplify the LC distribution into two fundamental types. One is “herbaceous”, without woody stems, found in the tundra to the north and grasslands to the south, one of the driest biomes of northern Eurasia. The second is “woody vegetation”, plants with woody stems, located within the area of boreal forests extending from west to east across much of the center of the domain (Fig. 1).

**2.1.2 Vegetation productivity – long term data**

Gross Primary Production (GPP) represents the total amount of carbon fixed per unit area by plants in an ecosystem utilizing the physiological process of photosynthesis (Watson et al., 2000). GPP is one the key metrics useful in assessments of changes in vegetation productivity. It is also a standard output of process-based vegetation models. As described by Yi et al. (2013) and Zhang et al. (2008), GPP is estimated in a manner similar to the MODIS MOD17 product (Running et al., 1999), using a Light Use Efficiency (LUE) approach similar to the MODIS (MOD17) productivity algorithm (Running et al., 2004). The model is driven by satellite-derived land cover, fractional photosynthetically active radiation (FPAR), and daily surface meteorology including incident solar radiation, minimum and average daily air temperatures and daylight vapor pressure deficit (VPD). In order to estimate FPAR using global biome-specific empirical relationships, NDVI was temporally interpolated to a daily time step (Yi et al., 2013). The LUE parameter for the conversion of photosynthetically active radiation to GPP accounts for reductions in photosynthesis under low temperatures and/or reductions in VPD due to daytime water stress. VPD is the only water constraint in the GPP model and assumes that VPD and plant-available soil moisture are in general equilibrium. For this GPP model, daily surface meteorology was drawn from the ERA-Interim dataset (Dee et al., 2011).

In this study, two datasets of satellite derived GPP are examined: (i) the third generation Global Inventory Modeling and Mapping Studies (GIMMS3g) (Zhu et al., 2013;

Pinzon and Tucker, 2010) and (ii) Vegetation Index and Phenology (VIP) (Didan, 2010; Barreto-Munoz, 2013) from the University of Arizona's Vegetation Index and Phenology Lab and made available under the NASA MEaSUREs (Making Earth System Data Records for Use in Research Environments) program. The GPP data are derived at a daily time step and then aggregated to a monthly time step for this study. They have a spatial resolution of 25 km, a temporal range from 1982 to 2010, and are restricted to the northern high latitudes ( $> 45^{\circ}$  N). Winter is characterized by extremely low productivity and technical problems of remote sensing make for a particular challenge in estimating GPP across the high latitudes (Pettorelli et al., 2005). In many of the statistical analyses to follow we use the ensemble mean of the two GPP datasets. Given the limited confidence in GPP data over winter (driven mainly by the uncertainty in winter NDVI) we focus on the remainder of the year in our analysis.

### 2.1.3 Flux tower data

To validate the observation based GPP data (derived using alternative GIMMS3g and VIP NDVI inputs using a LUE model), we used gap-filled daily tower GPP data at ten flux tower sites distributed across northern Eurasia, available for different periods of time. Details of the individual towers are provided in Table 1. The daily data was then aggregated to monthly and later to seasonal time step. The data, generated using the eddy covariance measurements acquired by the FLUXNET community, was collected from <http://www.fluxdata.org/> for the "Free Fair-Use" data subset. The spatial distribution of the flux towers used in this study is shown in Fig. 1. Unless otherwise noted we use seasonal totals of the daily gap-filled tower GPP data.

### 2.1.4 Temperature and precipitation

Monthly 2 m (m) air temperatures (in  $^{\circ}$ C) and precipitation (in  $\text{mm month}^{-1}$ ) data is drawn from a dataset developed by the University of Delaware (UDel). The product, at  $0.5^{\circ}$  resolution, was produced by interpolating meteorological station data with

**BGD**

12, 9121–9162, 2015

## Vegetation greening across northern Eurasia

P. Dass et al.

Title Page

Abstract

Introduction

Conclusions

References

Tables

Figures



Back

Close

Full Screen / Esc

Printer-friendly Version

Interactive Discussion



5 a method which accounts for the lapse rate in temperature with increasing elevation (Willmott and Matsuura, 1995). It also incorporates spatially high-resolution air temperature and precipitation climatologies (Willmott and Robeson, 1995). The database is available online (K. Matsuura and C. J. Willmott, Terrestrial air temperature: 1900–  
10 2008 gridded monthly time series, version 2.01, 2009, <http://climate.geog.udel.edu/~climate/>; C.J. Willmott and K. Matsuura, Terrestrial precipitation: 1900–2008 gridded monthly time series, version 2.01, 2009, <http://climate.geog.udel.edu/~climate/> Matsuura and Willmott, 2009). Although the GPP model does not use precipitation as an input, we assume that precipitation is a good measure of water supply to the vegetation and thus analyze it as one of the environmental variables affecting GPP. Here we use  
15 monthly values of temperature and precipitation for the period of 1982 to 2008, since this is the common period for which both GPP and the environmental variable data are available. Seasonal means for spring (March, April, May), summer (June, July, August), and autumn (September, October, November) are derived from the monthly values. As explained in SubSect. 2.1.2, lower reliability and availability of satellite NDVI observations and associated GPP data for the winter months leads us to focus on spring, summer, and autumn seasons.

### 2.1.5 Cloudiness

20 Cloudiness estimates are taken from monthly observations from meteorological stations, extending over the global land surface and interpolated onto a 0.5° grid (Mitchell and Jones, 2005). The dataset, CRU TS 2.1, is produced by the Climatic Research Unit (University of East Anglia) in conjunction with the Hadley Centre (at the UK Met Office), is available at <http://www.cru.uea.ac.uk/> (Harris et al., 2014).

### 2.1.6 Fire

25 Fire is represented by the burnt area (% of each grid cell) estimates from the Global Fire Emissions Database (GFED) Monthly Burned Area Data Set Version 3.1 released

**BGD**

12, 9121–9162, 2015

## **Vegetation greening across northern Eurasia**

P. Dass et al.

Title Page

Abstract

Introduction

Conclusions

References

Tables

Figures



Back

Close

Full Screen / Esc

Printer-friendly Version

Interactive Discussion



in April 2010. This product was developed on a global scale at a 0.5° spatial resolution and covers the period from 1997 to 2011. Primary satellite-based data source is the MODIS surface reflectance imagery (Giglio et al., 2010).

## 2.2 Methods

### 2.2.1 Validation

The GPP data derived using alternative GIMMS3g and VIP NDVI inputs using a LUE model are evaluated against the tower-based data after grids and temporal ranges of the satellite data derived GPP, corresponding to the respective ten flux towers have been extracted. The evaluation is carried out using three different approaches: (1) Pearson's product moment correlation, which is a measure of the linear dependence between simulated and observed values and its value ranges from  $-1$  to  $+1$  where 0 is no correlation and  $-1/+1$  is total negative or positive correlation respectively; (2) percent bias, which measures the average tendency of the simulated values to be larger or smaller than their observed ones. The optimal value is 0.0 with low-magnitude values indicating accurate model simulations. Positive values indicate overestimations and vice versa (Yapo et al., 1996; Sorooshian et al., 1993); (3) Nash–Sutcliffe efficiency (NSE) coefficient, which is a normalized statistic that determines the relative magnitude of the residual variance compared to the measured data variance (Nash and Sutcliffe, 1970). The statistic indicates how well the plot of observed vs. simulated data fits the 1 : 1 line. Nash–Sutcliffe efficiencies range from  $-\infty$  to 1. An efficiency of 1 corresponds to a perfect match of model simulated GPP to the observed data. An efficiency of 0 indicates that the model predictions are as accurate as the mean of the observed data, whereas an efficiency less than zero occurs when the observed mean is a better predictor than the model or, in other words, when the residual variance (between modeled and observed values), is larger than the data variance (between observed values and the observed mean). Essentially, the closer the model efficiency is to 1, the more accurate the model is.

## Vegetation greening across northern Eurasia

P. Dass et al.

Title Page

Abstract

Introduction

Conclusions

References

Tables

Figures



Back

Close

Full Screen / Esc

Printer-friendly Version

Interactive Discussion



## 2.2.2 Trend analysis

To quantify the influence of each environmental variable we apply a linear regression model to the respective time series. We derive these linear trends for each environmental variable and for GPP by calculating the trend slope at each grid cell ( $0.5^\circ \times 0.5^\circ$  area) across the study area. Both annual and seasonal time integrations are examined. Trends are deemed statistically significant at the 95 % level. Other studies have implemented a similar methodology to identify trends (Piao et al., 2011; de Jong et al., 2011; Forkel et al., 2013; Goetz et al., 2005). In order to determine whether the temporal rate of change differs for different periods of the study period we plot the percentage difference of the annual means (of the regional average) from that of the first 5 year mean. We then apply a smoothing function using the “smooth.spline” of the *R* language with a “spar” value of 0.8 (Chambers and Hastie, 1992; Green and Silverman, 1994; Hastie and Tibshirani, 1986).

Strong trends in the time series examined introduces the issue of collinearity due to the linear association between the variables. As a consequence, estimates of the influence of one variable on another become less precise. Therefore, de-trended series were used in the assessments of correlation coefficient and coefficients of determination.

## 2.2.3 Correlation

Correlation analysis is used to demonstrate the statistical dependence of one variable on another. We use the Karl Pearson’s product–moment correlation coefficient (represented as *R*), one of the more popular measures of dependence between two variables and which is sensitive only to a linear relationship between two variables. Pearson’s correlation coefficient is expressed from +1 (perfect increasing linear relationship) to –1 (perfect decreasing linear relationship or “inverse correlation”) and as the value approaches zero, the relationship is closer to being uncorrelated (Dowdy and Wearden, 1983).

**BGD**

12, 9121–9162, 2015

## **Vegetation greening across northern Eurasia**

P. Dass et al.

Title Page

Abstract

Introduction

Conclusions

References

Tables

Figures



Back

Close

Full Screen / Esc

Printer-friendly Version

Interactive Discussion



## 2.2.4 Attribution

The primary objective of this study is to determine the magnitude and spatio-temporal variations in trends for environmental conditions (variables) which have contributed to the change increase in GPP of northern Eurasia indicated from the satellite records. Ideally one would study the direct influence of one condition on another in experiments in which all other possible causes of variation are eliminated. However, since this study involves only large scale observational data and not process based models or laboratory based experiments, there is no control over the causes of variation. Investigations into the structure and function of terrestrial ecosystems, like those for many elements of the biological sciences, involve quantities which are often correlated. In some cases, the derived relationship may be spurious. The coefficient of determination (represented as  $R^2$ ) is a common measure to estimate the degree to which one variable can be explained by another (percentage) (Wright, 1921) while correlation analysis ( $R$ ) can explain this dependence of one variable on another keeping the sign of the relationship (+/-) intact (Aldrich, 1995).

## 3 Results and discussion

### 3.1 Validation of satellite derived GPP

The GPP data derived using alternative GIMMS3g and VIP NDVI inputs, as well as their ensemble mean are individually validated against the flux tower-based GPP data using Pearson's correlation coefficient, percent bias as well as the Nash–Sutcliffe normalized statistic. Table 2 lists the validation statistics by season. The correlation coefficients are positive and high ranging from 0.64 to 0.82. The correlation is highest for Spring. The percent bias is predominantly negative and lowest for Summer. Since all the values of the Nash–Sutcliffe Efficiencies are above zero, we can conclude that the modeled values are a more accurate estimate of the GPP than the observed mean for the re-

**BGD**

12, 9121–9162, 2015

## Vegetation greening across northern Eurasia

P. Dass et al.

Title Page

Abstract

Introduction

Conclusions

References

Tables

Figures



Back

Close

Full Screen / Esc

Printer-friendly Version

Interactive Discussion





and VIP datasets is discussed below. Examining the seasonality of GPP trends (mean GPP for the two datasets) (Fig. 3), we find that among the seasons the summer trend is greatest. This implies that the response of GPP to environmental changes is highest at the peak of the growing season. While GPP trends are predominantly positive, there are clearly areas each season with a negative trend.

The GPP increase described here is consistent with the results of Sitch et al. (2007), who also noted considerable interannual and spatial variability, with many areas demonstrating decreased greenness and lower productivity. Using a process based model (LPJ-DGVM) to perform a retrospective analysis for the period of 1982–1998, Lucht et al. (2002) found, after accounting for the carbon loss due to autotrophic respiration, that boreal zone NPP increased by  $34.6 \text{ g C m}^{-2} \text{ yr}^{-1}$ , higher than our estimate. The discrepancy may be due to the analysis of Lucht et al. (2002) ending in 1998, just prior to a decline in productivity from 2000–2008 as estimated from GIMMS GPP (Zhang et al., 2008; Buermann et al., 2014; Piao et al., 2011). The higher GPP trend in summer (Fig. 3) suggests that vegetation of this region is predominantly cold constrained, a finding described in other recent studies (Yi et al., 2013; Kim et al., 2014).

Uncertainty in ensemble mean GPP is illustrated by the coefficient of variation map (Fig. 2b). The highest uncertainty is noted in the north-central and the south-western part of the region. Accuracy of the GIMMS-NDVI dataset has been examined in several recent studies. Analyzing trends in growing season start over the Tibetan plateau, Zhang et al. (2013) found that GIMMS NDVI differed substantially over the period 2001–2006 from SPOT-VGT and MODIS-NDVIs. This deviation suggests severe data quality issues. The GIMMS dataset is based on the NOAA-AVHRR long term time series record, which is comprised of two different sensors, for two different time periods, which leads to the difficulty of among-instrument inter-calibration and complicates the use of AVHRR NDVI data in long-term time series trend analysis (Pinzon and Tucker, 2014). This leads, in turn, to the need for a seamless and consistent sensor-independent record of land surface vegetation index and phenology. Used here in parallel with the GIMMS3g dataset, the Vegetation Index and Phenology (VIP) dataset, whose data pro-

## BGD

12, 9121–9162, 2015

### Vegetation greening across northern Eurasia

P. Dass et al.

Title Page

Abstract

Introduction

Conclusions

References

Tables

Figures



Back

Close

Full Screen / Esc

Printer-friendly Version

Interactive Discussion



cessing applies a different correction scheme from that of GIMMS3g (Fensholt et al., 2015), is one such product. Available at <http://measures.arizona.edu>, it is produced through continuity algorithms which enable the seamless conversion of land surface vegetation records from AVHRR, MODIS and VIIRS (Didan, 2010).

### 3.3 Temporal changes in the environmental variables

The regionally averaged air temperature increase is nearly monotonic. Warming is highest in spring. More than half of the region is affected by a significant positive trend (Fig. 4a). Unlike temperature, precipitation does not exhibit a sustained increase over the 1982–2008 period. The precipitation trend is highest for summer (Fig. 4b), the peak of the growing season. This implies that precipitation trends have the potential to impact vegetation productivity indirectly since precipitation is not a direct input into the GPP model used in this study. Table 3 reveals the regional average of cloudiness to have a negative trend. However, similar to precipitation, the spatial standard deviation is more than 4 times the spatial mean, implying a high spatial variability and that the regional mean does not represent the trends of the whole region. Unlike precipitation, a greater fraction of the region sees a significant negative cloudiness trend or a significant clear sky trend. Burnt area has significant trends, both positive and negative, over only 1 % of the region with the total yearly burnt area for the study area increasing from 15.9 to 17.1 million hectares from 1997 to 2010. Based on the regional mean (Table 3; Fig. 4d), burnt area has a negative trend. However, a coefficient of variation of more than 20 suggests considerable uncertainty of the regional mean trend.

Recent studies and the IPCC Fourth Assessment Report (AR4) have reported similar changes in these environmental variables. Temperature trends over the region range from  $0.3\text{--}0.7\text{ }^{\circ}\text{C}10\text{yr}^{-1}$ . For most regions of the higher latitudes, especially from  $30$  to  $85^{\circ}\text{N}$ , significant positive precipitation trends have occurred (Trenberth et al., 2007). Contrary to the cloud cover trend we find here, studies reported in AR4 suggest an increased total cloud cover since the middle of the last century over many continental regions, including the former USSR and Western Europe (Sun et al., 2001; Sun and

BGD

12, 9121–9162, 2015

## Vegetation greening across northern Eurasia

P. Dass et al.

Title Page

Abstract

Introduction

Conclusions

References

Tables

Figures



Back

Close

Full Screen / Esc

Printer-friendly Version

Interactive Discussion



Groisman, 2000). The large spatial variability of the cloud cover trend (Table 3) may explain the disagreement. Burnt area data, representing fire, is dissimilar from the other environmental variables. It spans only 12 years of the 26 years, and is spatially non-uniform, involving only a fraction of the total study area. These characteristics make it difficult to assess impacts on vegetation productivity (Balshi et al., 2007). While the model used to generate the satellite NDVI derived GPP data does not account for CO<sub>2</sub> fertilization directly, this may be partially represented through associated changes in NDVI. However, as stated in Sect. 1, on account of the spatial homogeneity of atmospheric CO<sub>2</sub> concentration we do not include it in this in our statistical analysis.

### 3.4 Attributing GPP changes to environmental variables and assessing seasonality

With 3 of the 4 environmental variables studied, magnitude of the correlation (Fig. 5) as well as the explained variances (Table 4) for summer are highest among the seasons. This implies that the vegetation of northern Eurasia is most sensitive to environmental changes in summer, the peak of the growing season. For annual, spring and summer, not only are the explained variances for temperature are higher than the other variables, it is the only variable demonstrating a predominantly strong positive correlation with annual GPP. While the median explained variance for summer temperature is 33.3%, in contrast, it ranges between 2.2 and 11.8% by season and variable for the other variables. Moreover, 67.3% of the study area demonstrate significant positive correlation between GPP and temperature (Fig. 6, Table 5). This implies that, over recent decades, low temperatures have been the major constraint for GPP in northern Eurasia.

Similar results have been reported by Yi et al. (2014), who concluded that satellite derived vegetation indices show an overall benefit for summer photosynthetic activity from regional warming and only a limited impact from spring precipitation. The dominant constraint of temperature was described by Zhang et al. (2008), who found the same constraint to be decreasing. However, our results contrast with those of Piao

**BGD**

12, 9121–9162, 2015

## Vegetation greening across northern Eurasia

P. Dass et al.

Title Page

Abstract

Introduction

Conclusions

References

Tables

Figures



Back

Close

Full Screen / Esc

Printer-friendly Version

Interactive Discussion



et al. (2011), who concluded that at the continental scale of Eurasia, vegetation indices in summer are more strongly regulated by precipitation, while temperature is a relatively stronger regulator in spring and autumn. Regarding the dominance of temperature as a regulator, Yi et al. (2013) concluded that over the last decade, Eurasia has been more drought sensitive than other high latitude areas.

### 3.5 Stimulative and inhibitive effects of environmental variables on GPP

As described above, annual GPP is most sensitive to changes in the environmental variables in summer. We investigate this connection using de-trended annual GPP and the summer values of the de-trended environmental variables. The metric is Pearson's product moment correlation ( $R$ ). Box plots (Fig. 5) show the distributions. Correlations between annual GPP and summer air temperature are predominantly high and positive. For precipitation as well as cloud cover, the relationship with GPP is weak and negative, implying a predominantly inhibitory effect. Median of the correlation distribution for burnt area and GPP can not be distinguished from zero due to the high spatial variability. While high correlations provide an insight into the nature of the relationship, weak correlations reveal that the relationship is more complex, requiring analysis of additional environmental variables. For especially weaker correlations, spatial analyses reveal more about a relationship, as demonstrated below.

Map panels in Fig. 6 show the regions with statistically significant (95% significance level) correlations for summer values of each de-trended environmental variable and annual GPP. Table 5 lists the fraction of the region with significant correlations. While in 67.3% of northern Eurasia (see Table 5), increasing temperatures lead to increasing GPP (Fig. 6a), the southwestern part, which is dominated by grasslands (see Fig. 1) is characterized by strongly negative correlation (6.2% of the area) suggesting decreasing GPP with increasing temperatures for this area. This statistic coupled with the high explained variance for the temperature variable, implies that over recent decades, low temperatures have been the major constraint for GPP in most parts of northern Eurasia. This result is not surprising, as these grasslands are relatively dry compared to

## Vegetation greening across northern Eurasia

P. Dass et al.

[Title Page](#)

[Abstract](#)

[Introduction](#)

[Conclusions](#)

[References](#)

[Tables](#)

[Figures](#)



[Back](#)

[Close](#)

[Full Screen / Esc](#)

[Printer-friendly Version](#)

[Interactive Discussion](#)





greater drought sensitivity. Positive impacts of warming on GPP have been suggested in warming experiments (Natali et al., 2013). However, decreasing growing-season forest productivity, represented as “greenness” or other vegetation indices across northern Eurasia, may be a reflection of continued summer warming in the absence of sustained increases in precipitation (Buermann et al., 2014; Zhou et al., 2001). Wang et al. (2014) documented a positive relationship between sunshine duration (equivalent to the inverse of cloud cover) and vegetation greenness.

### 3.6 Relationships among individual environmental variables

Environmental variables are not independent of one another. We examine correlations among the individual variables to better understand their interactions. Figure 7 shows distributions of the various correlations. The temperature–precipitation correlation is predominantly negative, indicating that increases in precipitation did not accompany recent warming. These changes should lead to increasing water stress, which is only noted in a subset of the region. i.e. 4.4 and 2.3% of the area (GIMMS3g and VIP datasets) in the southern parts of the study area (Fig. 6a). The relationship between temperature and cloud cover is similar to that of temperature and precipitation, as well as precipitation and cloud cover (described below). The relationship between temperature and burnt area indicates, as expected, that warming leads to more forest fires. However this fails to explain the negative trend in burnt area. A positive trend in the severity (not accounted for by the burnt area metric), but not the extent of fires could explain the negative trend in burnt area.

Grid correlations between precipitation and cloud cover are predominately positive. Summer precipitation and annual GPP are negatively correlated in the north (Fig. 6b). This explains why spatial distributions of the correlation coefficients of precipitation and cloud cover with GPP are similar. While increasing cloud cover leads to an increased probability of precipitation (and thus reduces water stress), it also reduces the sunshine duration and thus GPP. The relationship between fire and precipitation and/or cloud

## BGD

12, 9121–9162, 2015

### Vegetation greening across northern Eurasia

P. Dass et al.

Title Page

Abstract

Introduction

Conclusions

References

Tables

Figures



Back

Close

Full Screen / Esc

Printer-friendly Version

Interactive Discussion



cover is predominantly negative, as increasing precipitation and/or cloud cover leads to increasing moisture availability, which inhibits fire.

Consistent with our results, Thompson et al. (2006) found that in the boreal and tundra regions of Alaska, NPP decreased when it was warmer and dryer and increased when it was warmer and wetter. Colder and wetter conditions also increased NPP. Yi et al. (2013) conclude that while globally, annual GPP for boreal forests is significantly higher in warmer years, the relationship does not hold true for Eurasian boreal forests, which they find to be more drought sensitive. Thus, regional GPP variations are more consistent with regional wetting and drying anomalies, as we note for the southwestern part of the study region. It should be noted that GPP refers only to above ground carbon exchange driven by photosynthesis. Other carbon cycle processes such as soil decomposition and heterotrophic respiration may not be responding in a similar manner. Additional studies are required before extrapolating these results to other carbon cycle components.

## 4 Conclusions

The ensemble mean of the GIMMS3g and VIP GPP datasets shows that vegetation productivity generally increased across northern Eurasia over the period 1982 to 2008, with a significant increase for 48.2 % of the region. A decrease in GPP occurred for 0.1 % of the region. We note some disagreement in the nature and magnitude of the increasing GPP among the two datasets. The regional mean trend for the ensemble mean GPP is  $2.4 (\pm 1.2) \text{ gCm}^{-2} \text{ month}^{-1} 10\text{yr}^{-1}$ . The grid analysis is consistent with results of prior studies which have suggested that air temperature is the dominant environmental variable influencing the increases in productivity across the northern high latitudes. Examining seasonality we find that for three out of the four environmental variables, the maximum effect on GPP is seen during summer. Considering the regional median  $R^2$ , summer air temperature explains 33.3 % of the variation in annual GPP. In contrast, the other environmental variables explain between 2.2 and 11.8 %.

## Vegetation greening across northern Eurasia

P. Dass et al.

Title Page

Abstract

Introduction

Conclusions

References

Tables

Figures



Back

Close

Full Screen / Esc

Printer-friendly Version

Interactive Discussion



**BGD**

12, 9121–9162, 2015

**Vegetation greening  
across northern  
Eurasia**

P. Dass et al.

[Title Page](#)[Abstract](#)[Introduction](#)[Conclusions](#)[References](#)[Tables](#)[Figures](#)[Back](#)[Close](#)[Full Screen / Esc](#)[Printer-friendly Version](#)[Interactive Discussion](#)

A significant positive correlation between summer air temperature and annual GPP is noted for 67.3 % of the region. For 6.2 % of the area, specifically the dryer grasslands in the southwest, temperature and GPP are inversely correlated. The remaining environmental variables also have a significant influence. Both precipitation and cloudiness show a predominantly negative correlation with GPP. Fire has a small effect, with only 4 % of the region showing a significant correlation, positive or negative, between burnt area and GPP. The spatial analysis reveals that the statistical relationships are not spatially homogeneous. While warming likely contributed to increasing productivity across much of northern Eurasia, the relationship reverses in the southern grasslands which are relatively dry. This region exhibits increasing GPP, with warming having occurred without an increase in precipitation. This result demonstrates that vegetation has been resilient to drought stress. However if temperatures were to increase without precipitation meeting the higher atmospheric demand, the region may experience increasing drought stress over time.

The scientific method to analyze attribution of temporal changes in GPP is to conduct experiments where only a single factor (or environmental driver) is allowed to change temporally while other factors are kept constant (Wright, 1921). Since this is difficult to achieve using observation data, it is recommended that this study be followed up with experiments conducted using process-based models in which a single forcing variable independent of the others is manipulated. If feasible, multiple models should be used in order to quantify the uncertainty due to differences in model parameterization. Depending on emissions, population and other forcing scenarios, rates of change in the environmental drivers such as air temperature and precipitation may be different than those found in this study. Thus it is critical to examine future scenarios of change across the region to better understand terrestrial vegetation dynamics under the respective model simulations. The environmental drivers influence other elements of the carbon cycle beyond terrestrial vegetation. In order to determine how terrestrial carbon stocks and fluxes have changed in the recent past, or may change in the near

future, all aspects of the carbon cycle should be investigated in the context of changes in overarching climate influences.

*Acknowledgements.* This research was supported by the U.S. National Aeronautics and Space Administration NASA grant NNX11AR16G and the Permafrost Carbon Network (<http://www.permafrostcarbon.org/>) funded by the National Science Foundation. The MODIS Land Cover Type product data was obtained through the online Data Pool at the NASA Land Processes Distributed Active Archive Center (LP DAAC), USGS/Earth Resources Observation and Science (EROS) Center, Sioux Falls, South Dakota ([https://lpdaac.usgs.gov/data\\_access](https://lpdaac.usgs.gov/data_access)). We thank the researchers working at FLUXNET sites for making available their CO<sub>2</sub> flux data.

## References

- Ainsworth, E. A. and Long, S. P.: What have we learned from 15 years of free-air CO<sub>2</sub> enrichment (FACE)? A meta-analytic review of the responses of photosynthesis, canopy properties and plant production to rising CO<sub>2</sub>, *New Phytol.*, 165, 351–372, doi:10.1111/j.1469-8137.2004.01224.x, 2005. 9124
- Aldrich, J.: Correlations genuine and spurious in Pearson and Yule, *Stat. Sci.*, 10, 364–376, 1995. 9131
- Alton, P. B., North, P. R., and Los, S. O.: The impact of diffuse sunlight on canopy light-use efficiency, gross photosynthetic product and net ecosystem exchange in three forest biomes, *Glob. Change Biol.*, 13, 776–787, doi:10.1111/j.1365-2486.2007.01316.x, 2007. 9137
- Amiro, B. D., Chen, J. M., and Liu, J.: Net primary productivity following forest fire for Canadian ecoregions, *Can. J. Forest Res.*, 30, 939–947, doi:10.1139/x00-025, 2000. 9124
- Balshi, M. S., McGuire, A. D., Zhuang, Q., Melillo, J., Kicklighter, D. W., Kasischke, E., Wirth, C., Flannigan, M., Harden, J., Clein, J. S., Burnside, T. J., McAllister, J., Kurz, W. A., Apps, M., and Shvidenko, A.: The role of historical fire disturbance in the carbon dynamics of the pan-boreal region: a process-based analysis, *J. Geophys. Res.-Biogeo.*, 112, G02029, doi:10.1029/2006JG000380, 2007. 9135
- Barreto-Munoz, A.: Multi-Sensor Vegetation Index and Land Surface Phenology Earth Science Data Records in Support of Global Change Studies: Data Quality Challenges and Data Explorer System, available at: <http://arizona.openrepository.com/arizona/handle/10150/301661> (last access: 19 May 2015), 2013. 9127

## Vegetation greening across northern Eurasia

P. Dass et al.

Title Page

Abstract

Introduction

Conclusions

References

Tables

Figures



Back

Close

Full Screen / Esc

Printer-friendly Version

Interactive Discussion



## Vegetation greening across northern Eurasia

P. Dass et al.

Title Page

Abstract

Introduction

Conclusions

References

Tables

Figures



Back

Close

Full Screen / Esc

Printer-friendly Version

Interactive Discussion



- Berner, L. T., Beck, P. S. A., Bunn, A. G., Lloyd, A. H., and Goetz, S. J.: High-latitude tree growth and satellite vegetation indices: correlations and trends in Russia and Canada (1982–2008), *J. Geophys. Res.-Biogeo.*, 116, G01015, doi:10.1029/2010JG001475, 2011. 9132
- Blasing, T.: Recent Greenhouse Gas Concentrations, Tech. rep., available at: [http://cdiac.ornl.gov/pns/current\\_ghg.html](http://cdiac.ornl.gov/pns/current_ghg.html) (last access: 30 January 2015), 2009. 9124
- Bowes, G.: Photosynthetic responses to changing atmospheric carbon dioxide concentration, in: *Photosynthesis and the Environment*, 387–407, Springer, the Netherlands, 1996. 9123
- Buermann, W., Bikash, P. R., Jung, M., Burn, D. H., and Reichstein, M.: Earlier springs decrease peak summer productivity in North American boreal forests, *Environ. Res. Lett.*, 8, 024027, doi:10.1088/1748-9326/8/2/024027, 2013. 9124
- Buermann, W., Parida, B., Jung, M., MacDonald, G. M., Tucker, C. J., and Reichstein, M.: Recent shift in Eurasian boreal forest greening response may be associated with warmer and drier summers, *Geophys. Res. Lett.*, 41, GL059450, doi:10.1002/2014GL059450, 2014. 9124, 9133, 9138
- Carlson, T. N. and Ripley, D. A.: On the relation between NDVI, fractional vegetation cover, and leaf area index, *Remote Sens. Environ.*, 62, 241–252, doi:10.1016/S0034-4257(97)00104-1, 1997. 9122
- Chambers, J. M. and Hastie, T.: *Statistical Models in S*, Chapman and Hall, London, 1992. 9130
- de Jong, R., de Bruin, S., de Wit, A., Schaepman, M. E., and Dent, D. L.: Analysis of monotonic greening and browning trends from global NDVI time-series, *Remote Sens. Environ.*, 115, 692–702, doi:10.1016/j.rse.2010.10.011, 2011. 9130
- Dee, D. P., Uppala, S. M., Simmons, A. J., Berrisford, P., Poli, P., Kobayashi, S., Andrae, U., Balmaseda, M. A., Balsamo, G., Bauer, P., Bechtold, P., Beljaars, A. C. M., van de Berg, L., Bidlot, J., Bormann, N., Delsol, C., Dragani, R., Fuentes, M., Geer, A. J., Haimberger, L., Healy, S. B., Hersbach, H., Hólm, E. V., Isaksen, I., Kållberg, P., Köhler, M., Matricardi, M., McNally, A. P., Monge-Sanz, B. M., Morcrette, J.-J., Park, B.-K., Peubey, C., de Rosnay, P., Tavolato, C., Thépaut, J.-N., and Vitart, F.: The ERA-Interim reanalysis: configuration and performance of the data assimilation system, *Q. J. Roy. Meteor. Soc.*, 137, 553–597, doi:10.1002/qj.828, 2011. 9126
- Didan, K.: Multi-Satellite Earth Science Data Record for Studying Global Vegetation Trends and Changes, in: *Proceedings of the 2010 International Geoscience and Remote Sensing Symposium*, 25–30 July 2010, Honolulu, HI, USA, 25–30, 2010. 9127, 9134

## Vegetation greening across northern Eurasia

P. Dass et al.

Title Page

Abstract

Introduction

Conclusions

References

Tables

Figures



Back

Close

Full Screen / Esc

Printer-friendly Version

Interactive Discussion



- Dowdy, S. and Wearden, S.: Statistics for Research, Wiley Series in Probability and Mathematical Statistics, John Wiley & Sons, New York, USA, 1983. 9130
- Fensholt, R., Horion, S., Tagesson, T., Ehammer, A., Grogan, K., Tian, F., Huber, S., Verbesselt, J., Prince, S. D., Tucker, C. J., and Rasmussen, K.: Assessment of vegetation trends in drylands from time series of earth observation data, in: Remote Sensing Time Series, edited by: Kuenzer, C., Dech, S., and Wagner, W., no. 22 in Remote Sensing and Digital Image Processing, 159–182, Springer International Publishing, Cham, Switzerland, available at: [http://link.springer.com/chapter/10.1007/978-3-319-15967-6\\_8](http://link.springer.com/chapter/10.1007/978-3-319-15967-6_8) (last access: 19 May 2015), 2015. 9134
- Forkel, M., Carvalhais, N., Verbesselt, J., Mahecha, M. D., Neigh, C. S. R., and Reichstein, M.: Trend change detection in NDVI time series: effects of inter-annual variability and methodology, *Remote Sensing*, 5, 2113–2144, doi:10.3390/rs5052113, 2013. 9130
- Friedl, M. A., McIver, D. K., Hodges, J. C. F., Zhang, X. Y., Muchoney, D., Strahler, A. H., Woodcock, C. E., Gopal, S., Schneider, A., Cooper, A., Baccini, A., Gao, F., and Schaaf, C.: Global land cover mapping from MODIS: algorithms and early results, *Remote Sens. Environ.*, 83, 287–302, doi:10.1016/S0034-4257(02)00078-0, 2002. 9125, 9156
- Gates, D. M.: Leaf Temperature and Transpiration, *Agron. J.*, 56, 273, doi:10.2134/agronj1964.00021962005600030007x, 1964. 9137
- Giglio, L., Randerson, J. T., van der Werf, G. R., Kasibhatla, P. S., Collatz, G. J., Morton, D. C., and DeFries, R. S.: Assessing variability and long-term trends in burned area by merging multiple satellite fire products, *Biogeosciences*, 7, 1171–1186, doi:10.5194/bg-7-1171-2010, 2010. 9129, 9159
- Goetz, S. J., Bunn, A. G., Fiske, G. J., and Houghton, R. A.: Satellite-observed photosynthetic trends across boreal North America associated with climate and fire disturbance, *P. Natl. Acad. Sci. USA*, 102, 13521–13525, doi:10.1073/pnas.0506179102, 2005. 9124, 9130
- Graven, H. D., Keeling, R. F., Piper, S. C., Patra, P. K., Stephens, B. B., Wofsy, S. C., Welp, L. R., Sweeney, C., Tans, P. P., Kelley, J. J., Daube, B. C., Kort, E. A., Santoni, G. W., and Bent, J. D.: Enhanced seasonal exchange of CO<sub>2</sub> by northern ecosystems since 1960, *Science*, 341, 1085–1089, doi:10.1126/science.1239207, 2013. 9123, 9124
- Green, P. J. and Silverman, B. W.: Nonparametric regression and generalized linear models: a roughness penalty approach, Chapman and Hall, London, 1994. 9130

## Vegetation greening across northern Eurasia

P. Dass et al.

Title Page

Abstract

Introduction

Conclusions

References

Tables

Figures



Back

Close

Full Screen / Esc

Printer-friendly Version

Interactive Discussion



Groisman, P. Y. and Bartalev, S. A.: Northern Eurasia earth science partnership initiative (NEESPI), science plan overview, *Global Planet. Change*, 56, 215–234, doi:10.1016/j.gloplacha.2006.07.027, 2007. 9125

Groisman, P. Y., Koknaeva, V. V., Belokrylova, T. A., and Karl, T. R.: Overcoming biases of precipitation measurement: a history of the USSR experience, *B. Am. Meteorol. Soc.*, 72, 1725–1733, doi:10.1175/1520-0477(1991)072<1725:OBOPMA>2.0.CO;2, 1991. 9123

Gu, L., Baldocchi, D., Verma, S. B., Black, T. A., Vesala, T., Falge, E. M., and Dowty, P. R.: Advantages of diffuse radiation for terrestrial ecosystem productivity, *J. Geophys. Res.-Atmos.*, 107, ACL 2–1, doi:10.1029/2001JD001242, 2002. 9137

Guay, K. C., Beck, P. S., Berner, L. T., Goetz, S. J., Baccini, A., and Buermann, W.: Vegetation productivity patterns at high northern latitudes: a multi-sensor satellite data assessment, *Glob. Change Biol.*, 20, 3147–3158, doi:10.1111/gcb.12647, 2014. 9122, 9124

Harris, I., Jones, P., Osborn, T., and Lister, D.: Updated high-resolution grids of monthly climatic observations – the CRU TS3.10 Dataset, *Int. J. Climatol.*, 34, 623–642, doi:10.1002/joc.3711, 2014. 9128, 9159

Hastie, T. and Tibshirani, R.: *Generalized additive models*, Chapman and Hall, London, 1986. 9130

Hickler, T., Smith, B., Prentice, I. C., Mjöfors, K., Miller, P., Arneth, A., and Sykes, M. T.: CO<sub>2</sub> fertilization in temperate FACE experiments not representative of boreal and tropical forests, *Glob. Change Biol.*, 14, 1531–1542, doi:10.1111/j.1365-2486.2008.01598.x, 2008. 9124

Jackson, R. D., Idso, S. B., Reginato, R. J., and Pinter, P. J.: Canopy temperature as a crop water stress indicator, *Water Resour. Res.*, 17, 1133–1138, doi:10.1029/WR017i004p01133, 1981. 9137

Johnstone, J. F. and Kasischke, E. S.: Stand-level effects of soil burn severity on postfire regeneration in a recently burned black spruce forest, *Can. J. Forest Res.*, 35, 2151–2163, doi:10.1139/x05-087, 2005. 9137

Kim, Y., Kimball, J., Zhang, K., Didan, K., Velicogna, I., and McDonald, K.: Attribution of divergent northern vegetation growth responses to lengthening non-frozen seasons using satellite optical-NIR and microwave remote sensing, *Int. J. Remote Sens.*, 35, 3700–3721, doi:10.1080/01431161.2014.915595, 2014. 9123, 9124, 9133

Larcher, W.: Effect of environmental and physiological variables on the carbon dioxide gas exchange of trees, *Photosynthetica*, 3, 167–198, 1969. 9123

- Larcher, W.: *Physiological Plant Ecology: Ecophysiology and Stress Physiology of Functional Groups*, Springer, Berlin, Germany, 2003. 9123
- Lecomte, N., Simard, M., and Bergeron, Y.: Effects of fire severity and initial tree composition on stand structural development in the coniferous boreal forest of northwestern Québec, Canada, *Ecoscience*, 13, 152–163, doi:10.2980/i1195-6860-13-2-152.1, 2006. 9137
- Lucht, W., Prentice, I. C., Myneni, R. B., Sitch, S., Friedlingstein, P., Cramer, W., Bousquet, P., Buermann, W., and Smith, B.: Climatic control of the high-latitude vegetation greening trend and Pinatubo effect, *Science*, 296, 1687–1689, doi:10.1126/science.1071828, 2002. 9133
- Matsuura, K. and Willmott, C. J.: *Terrestrial Precipitation: 1900–2008 Gridded Monthly Time Series*, Center for Climatic Research Department of Geography Center for Climatic Research, University of Delaware, Newark, DE, USA, 2009. 9128, 9159
- Mitchell, T. D. and Jones, P. D.: An improved method of constructing a database of monthly climate observations and associated high-resolution grids, *Int. J. Climatol.*, 25, 693–712, doi:10.1002/joc.1181, 2005. 9128
- Myneni, R. B., Keeling, C. D., Tucker, C. J., Asrar, G., and Nemani, R. R.: Increased plant growth in the northern high latitudes from 1981 to 1991, *Nature*, 386, 698–702, doi:10.1038/386698a0, 1997. 9122, 9123, 9124
- Nash, J. E. and Sutcliffe, J. V.: River flow forecasting through conceptual models part I – A discussion of principles, *J. Hydrol.*, 10, 282–290, doi:10.1016/0022-1694(70)90255-6, 1970. 9129, 9152
- Natali, S. M., Schuur, E. A. G., Webb, E. E., Pries, C. E. H., and Crummer, K. G.: Permafrost degradation stimulates carbon loss from experimentally warmed tundra, *Ecology*, 95, 602–608, doi:10.1890/13-0602.1, 2013. 9138
- Nemani, R. R., Keeling, C. D., Hashimoto, H., Jolly, W. M., Piper, S. C., Tucker, C. J., Myneni, R. B., and Running, S. W.: Climate-driven increases in global terrestrial net primary production from 1982 to 1999, *Science*, 300, 1560–1563, doi:10.1126/science.1082750, 2003. 9124, 9137
- Nicholls, N., Gruza, G., Jouzel, J., Karl, T., Ogallo, L., and Parker, D.: *Observed climate variability and change*, Cambridge University Press, New York, USA and Melbourne, Australia, 1996. 9123
- Overpeck, J., Hughen, K., Hardy, D., Bradley, R., Case, R., Douglas, M., Finney, B., Gajewski, K., Jacoby, G., Jennings, A., Lamoureux, S., Lasca, A., MacDonald, G., Moore, J.,

**Vegetation greening  
across northern  
Eurasia**

P. Dass et al.

Title Page

Abstract

Introduction

Conclusions

References

Tables

Figures



Back

Close

Full Screen / Esc

Printer-friendly Version

Interactive Discussion



## Vegetation greening across northern Eurasia

P. Dass et al.

Title Page

Abstract

Introduction

Conclusions

References

Tables

Figures



Back

Close

Full Screen / Esc

Printer-friendly Version

Interactive Discussion



- Retelle, M., Smith, S., Wolfe, A., and Zielinski, G.: Arctic environmental change of the last four centuries, *Science*, 278, 1251–1256, doi:10.1126/science.278.5341.1251, 1997. 9123
- Parida, B. R. and Buermann, W.: Increasing summer drying in North American ecosystems in response to longer nonfrozen periods, *Geophys. Res. Lett.*, 41, 2014GL060495, doi:10.1002/2014GL060495, 2014. 9124
- Pettorelli, N., Vik, J. O., Mysterud, A., Gaillard, J.-M., Tucker, C. J., and Stenseth, N. C.: Using the satellite-derived NDVI to assess ecological responses to environmental change, *Trends Ecol. Evol.*, 20, 503–510, doi:10.1016/j.tree.2005.05.011, 2005. 9127
- Piao, S., Wang, X., Ciais, P., Zhu, B., Wang, T., and Liu, J.: Changes in satellite-derived vegetation growth trend in temperate and boreal Eurasia from 1982 to 2006, *Glob. Change Biol.*, 17, 3228–3239, doi:10.1111/j.1365-2486.2011.02419.x, 2011. 9130, 9133, 9135
- Pinzon, J. E. and Tucker, C. J.: GIMMS 3g NDVI set and global NDVI trends, in: *Second Yamal Land-Cover Land-Use Change Workshop Arctic Centre (Rovaniemi, March), 2010*. 9127
- Pinzon, J. E. and Tucker, C. J.: A non-stationary 1981–2012 AVHRR NDVI3g time series, *Remote Sensing*, 6, 6929–6960, doi:10.3390/rs6086929, 2014. 9133
- Raynolds, M. K., Walker, D. A., Epstein, H. E., Pinzon, J. E., and Tucker, C. J.: A new estimate of tundra-biome phytomass from trans-Arctic field data and AVHRR NDVI, *Remote Sensing Letters*, 3, 403–411, doi:10.1080/01431161.2011.609188, 2012. 9132
- Reich, P. B., Peterson, D. W., Wedin, D. A., and Wrage, K.: Fire and vegetation effects on productivity and nitrogen cycling across a forest–grassland continuum, *Ecology*, 82, 1703–1719, doi:10.1890/0012-9658(2001)082[1703:FAVEOP]2.0.CO;2, 2001. 9124
- Richards, F. and Arkin, P.: On the relationship between satellite-observed cloud cover and precipitation, *Mon. Weather Rev.*, 109, 1081–1093, doi:10.1175/1520-0493(1981)109<1081:OTRBSO>2.0.CO;2, 1981. 9137
- Roderick, M. L., Farquhar, G. D., Berry, S. L., and Noble, I. R.: On the direct effect of clouds and atmospheric particles on the productivity and structure of vegetation, *Oecologia*, 129, 21–30, doi:10.1007/s004420100760, 2001. 9124, 9137
- Running, S. W., Nemani, R., Glassy, J. M., and Thornton, P. E.: MODIS daily photosynthesis (PSN) and annual net primary production (NPP) product (MOD17): Algorithm Theoretical Basis Document, University of Montana, SCF At-Launch Algorithm ATBD Documents, available at: <http://www.nts.g.umt.edu/project/MOD17/> (last access: 16 June 2015), 1999. 9126

## Vegetation greening across northern Eurasia

P. Dass et al.

Title Page

Abstract

Introduction

Conclusions

References

Tables

Figures



Back

Close

Full Screen / Esc

Printer-friendly Version

Interactive Discussion



- Running, S. W., Nemani, R. R., Heinsch, F. A., Zhao, M., Reeves, M., and Hashimoto, H.: A continuous satellite-derived measure of global terrestrial primary production, *Bioscience*, 54, 547–560, doi:10.1641/0006-3568(2004)054[0547:ACSMOG]2.0.CO;2, 2004. 9126
- Rötter, R., and Geijn, S. C. v. d.: Climate change effects on plant growth, crop yield and live-stock, *Climatic Change*, 43, 651–681, doi:10.1023/A:1005541132734, 1999. 9123
- Sharp, R. E., Poroyko, V., Hejlek, L. G., Spollen, W. G., Springer, G. K., Bohnert, H. J., and Nguyen, H. T.: Root growth maintenance during water deficits: physiology to functional ge-nomics, *J. Exp. Bot.*, 55, 2343–2351, 2004. 9123
- Shim, C., Hong, J., Hong, J., Kim, Y., Kang, M., Malla Thakuri, B., Kim, Y., and Chun, J.: Evalu-ation of MODIS GPP over a complex ecosystem in East Asia: a case study at Gwangneung flux tower in Korea, *Adv. Space Res.*, 54, 2296–2308, doi:10.1016/j.asr.2014.08.031, 2014. 9137
- Sitch, S., McGuire, A. D., Kimball, J., Gedney, N., Gamon, J., Engstrom, R., Wolf, A., Zhuang, Q., Clein, J., and McDonald, K. C.: Assessing the carbon balance of circumpolar Arctic tundra using remote sensing and process modeling, *Ecol. Appl.*, 17, 213–234, 2007. 9133
- Sorooshian, S., Duan, Q., and Gupta, V. K.: Calibration of rainfall-runoff models: application of global optimization to the Sacramento Soil Moisture Accounting Model, *Water Resour. Res.*, 29, 1185–1194, doi:10.1029/92WR02617, 1993. 9129, 9152
- Stevens, C. J., Dise, N. B., Mountford, J. O., and Gowing, D. J.: Impact of nitrogen deposition on the species richness of grasslands, *Science*, 303, 1876–1879, 2004. 9123
- Sun, B. and Groisman, P. Y.: Cloudiness variations over the former Soviet Union, *Int. J. Clima-tol.*, 20, 1097–1111, 2000. 9134
- Sun, B., Groisman, P. Y., and Mokhov, I. I.: Recent changes in cloud-type frequency and inferred increases in convection over the United States and the former USSR, *J. Climate*, 14, 1864–1880, 2001. 9134
- Thompson, C. C., McGuire, A. D., Clein, J. S., Iii, F. S. C., and Beringer, J.: Net carbon exchange across the Arctic tundra-boreal forest transition in Alaska 1981–2000, *Mitigation and Adap-tation Strategies for Global Change*, 11, 805–827, doi:10.1007/s11027-005-9016-3, 2006. 9124, 9139
- Trenberth, K. E., Jones, P. D., Ambenje, P., Bojariu, R., Easterling, D., Klein Tank, A., Parker, D., Rahimzadeh, F., Renwick, J. A., Rusticucci, M., Soden, B., Zhai, P., Adler, R., Alexander, L., Allan, R., Baldwin, M. P., Beniston, M., Bromwich, D., Camilloni, I., Cassou, C., Cayan, D. R.,

## Vegetation greening across northern Eurasia

P. Dass et al.

Title Page

Abstract

Introduction

Conclusions

References

Tables

Figures



Back

Close

Full Screen / Esc

Printer-friendly Version

Interactive Discussion



Chang, E. K. M., Christy, J., Dai, A., Deser, C., Dotzek, N., Fasullo, J., Fogt, R., Folland, C., Forster, P., Free, M., Frei, C., Gleason, B., Grieser, J., Groisman, P., Gulev, S., Hurrell, J., Ishii, M., Josey, S., Kållberg, P., Kennedy, J., Kiladis, G., Kripalani, R., Kunkel, K., Lam, C.-Y., Lanzante, J., Lawrimore, J., Levinson, D., Liepert, B., Norris, G., Oki, T., Robertson, F. R., Rosenlof, K., Semazzi, F. H., Shea, D., Shepherd, J. M., Shepherd, T. G., Sherwood, S., Siegmund, P., Simmonds, I., Simmons, A., Thorncroft, C., Thorne, P., Uppala, S., Vose, R., Wang, B., Warren, S., Washington, R., Wheeler, M., Wielicki, B., Wong, T., and Wuertz, D.: Observations: surface and atmospheric climate change, in: *Climate Change 2007: The Physical Science Basis, Contribution of Working Group 1 to the Fourth Assessment Report of the Intergovernmental Panel on Climate Change*, 235–336, Cambridge University Press, Cambridge, UK and NY, USA, available at: [http://www.ipcc.ch/publications\\_and\\_data/ar4/wg1/en/ch3.html](http://www.ipcc.ch/publications_and_data/ar4/wg1/en/ch3.html) (last access: 16 June 2015), 2007. 9134

Urban, M., Forkel, M., Eberle, J., Hüttich, C., Schmullius, C., and Herold, M.: Pan-Arctic climate and land cover trends derived from multi-variate and multi-scale analyses (1981–2012), *Remote Sensing*, 6, 2296–2316, 2014. 9123, 9124

Walker, X. J., Mack, M. C., and Johnstone, J. F.: Stable carbon isotope analysis reveals widespread drought stress in boreal black spruce forests, *Glob. Change Biol.*, doi:10.1111/gcb.12893, 2015. 9124

Wang, H., Liu, D., Lin, H., Montenegro, A., and Zhu, X.: NDVI and vegetation phenology dynamics under the influence of sunshine duration on the Tibetan plateau, *Int. J. Climatol.*, 35, 687–698, doi:10.1002/joc.4013, 2014. 9138

Watson, R., Noble, I., Bolin, B., Ravindranath, N., Verardo, D., and Dokken, D.: Land use, land-use change and forestry: a special report of the Intergovernmental Panel on Climate Change, Cambridge University Press, Cambridge, England, available at: [http://www.ipcc.ch/ipccreports/sres/land\\_use/](http://www.ipcc.ch/ipccreports/sres/land_use/) (last access: 16 June 2015), 2000. 9126

Wiegand, C. L. and Namken, L. N.: Influences of Plant Moisture Stress, Solar Radiation, and Air Temperature on Cotton Leaf Temperature, *Agron. J.*, 58, 582, doi:10.2134/agronj1966.00021962005800060009x, 1966. 9137

Williams, M., Rastetter, E. B., Van der Pol, L., and Shaver, G. R.: Arctic canopy photosynthetic efficiency enhanced under diffuse light, linked to a reduction in the fraction of the canopy in deep shade, *New Phytol.*, 202, 1267–1276, doi:10.1111/nph.12750, 2014. 9137

## Vegetation greening across northern Eurasia

P. Dass et al.

[Title Page](#)

[Abstract](#)

[Introduction](#)

[Conclusions](#)

[References](#)

[Tables](#)

[Figures](#)



[Back](#)

[Close](#)

[Full Screen / Esc](#)

[Printer-friendly Version](#)

[Interactive Discussion](#)



Willmott, C. J. and Matsuura, K.: Smart interpolation of annually averaged air temperature in the United States, *J. Appl. Meteorol.*, 34, 2577–2586, doi:10.1175/1520-0450(1995)034<2577:SIOAAA>2.0.CO;2, 1995. 9128

Willmott, C. J. and Robeson, S. M.: Climatologically aided interpolation (CAI) of terrestrial air temperature, *Int. J. Climatol.*, 15, 221–229, doi:10.1002/joc.3370150207, 1995. 9128

Wright, S.: Correlation and causation, *J. Agric. Res.*, 20, 557–585, 1921. 9131, 9140

Yapo, P. O., Gupta, H. V., and Sorooshian, S.: Automatic calibration of conceptual rainfall-runoff models: sensitivity to calibration data, *J. Hydrol.*, 181, 23–48, doi:10.1016/0022-1694(95)02918-4, 1996. 9129, 9152

Yi, C., Ricciuto, D., Li, R., Wolbeck, J., Xu, X., Nilsson, M., Aires, L., Albertson, J. D., Ammann, C., Arain, M. A., Araujo, A. C. d., Aubinet, M., Aurela, M., Barcza, Z., Barr, A., Berbigier, P., Beringer, J., Bernhofer, C., Black, A. T., Bolstad, P. V., Bosveld, F. C., Broadmeadow, M. S. J., Buchmann, N., Burns, S. P., Cellier, P., Chen, J., Chen, J., Ciais, P., Clement, R., Cook, B. D., Curtis, P. S., Dail, D. B., Dellwik, E., Delpierre, N., Desai, A. R., Dore, S., Dragoni, D., Drake, B. G., Dufrene, E., Dunn, A., Elbers, J., Eugster, W., Falk, M., Feigenwinter, C., Flanagan, L. B., Foken, T., Frank, J., Fuhrer, J., Gianelle, D., Goldstein, A., Goulden, M., Granier, A., Grunwald, T., Gu, L., Guo, H., Hammerle, A., Han, S., Hanan, N. P., Haszpra, L., Heinesch, B., Helfter, C., Hendriks, D., Hutley, L. B., Ibrom, A., Jacobs, C., Johansson, T., Jongen, M., Katul, G., Kiely, G., Klumpp, K., Knohl, A., Kolb, T., Kutsch, W. L., Lafleur, P., Laurila, T., Leuning, R., Lindroth, A., Liu, H., Loubet, B., Manca, G., Marek, M., Margolis, H. A., Martin, T. A., Massman, W. J., Matamala, R., Matteucci, G., McCaughey, H., Merbold, L., Meyers, T., Migliavacca, M., Miglietta, F., Misson, L., Molder, M., Moncrieff, J., Monson, R. K., Montagnani, L., Montes-Helu, M., Moors, E., Moureaux, C., Mukelabai, M. M., Munger, J. W., Myklebust, M., Nagy, Z., Noormets, A., Oechel, W., Oren, R., Pallardy, S. G., U, K. T. P., Pereira, J. S., Pilegaard, K., Pinter, K., Pio, C., Pita, G., Powell, T. L., Rambal, S., Randerson, J. T., Randow, C. v., Rebmann, C., Rinne, J., Rossi, F., Roulet, N., Ryel, R. J., Sagerfors, J., Saigusa, N., Sanz, M. J., Mugnozza, G.-S., Schmid, H. P., Seufert, G., Siqueira, M., Soussana, J.-F., Starr, G., Sutton, M. A., Tenhunen, J., Tuba, Z., Tuovinen, J.-P., Valentini, R., Vogel, C. S., Wang, J., Wang, S., Wang, W., Welp, L. R., Wen, X., Wharton, S., Wilkinson, M., Williams, C. A., Wohlfahrt, G., Yamamoto, S., Yu, G., Zampedri, R., Zhao, B., and Zhao, X.: Climate control of terrestrial carbon exchange across biomes and continents, *Environ. Res. Lett.*, 5, 034007, doi:10.1088/1748-9326/5/3/034007, 2010. 9124

## Vegetation greening across northern Eurasia

P. Dass et al.

Title Page

Abstract

Introduction

Conclusions

References

Tables

Figures



Back

Close

Full Screen / Esc

Printer-friendly Version

Interactive Discussion



- Yi, Y., Kimball, J. S., Jones, L. A., Reichle, R. H., Nemani, R., and Margolis, H. A.: Recent climate and fire disturbance impacts on boreal and arctic ecosystem productivity estimated using a satellite-based terrestrial carbon flux model, *J. Geophys. Res.-Biogeo.*, 118, 606–622, doi:10.1002/jgrg.20053, 2013. 9124, 9126, 9132, 9133, 9136, 9137, 9139
- 5 Yi, Y., Kimball, J. S., and Reichle, R. H.: Spring hydrology determines summer net carbon uptake in northern ecosystems, *Environ. Res. Lett.*, 9, 064003, doi:10.1088/1748-9326/9/6/064003, 2014. 9135
- Zhang, G., Zhang, Y., Dong, J., and Xiao, X.: Green-up dates in the Tibetan Plateau have continuously advanced from 1982 to 2011, *P. Natl. Acad. Sci. USA*, 110, 4309–4314, doi:10.1073/pnas.1210423110, 2013. 9133
- 10 Zhang, K., Kimball, J. S., Hogg, E. H., Zhao, M., Oechel, W. C., Cassano, J. J., and Running, S. W.: Satellite-based model detection of recent climate-driven changes in northern high-latitude vegetation productivity, *J. Geophys. Res.-Biogeo.*, 113, G03033, doi:10.1029/2007JG000621, 2008. 9124, 9126, 9132, 9133, 9135, 9137
- 15 Zhou, L., Tucker, C. J., Kaufmann, R. K., Slayback, D., Shabanov, N. V., and Myneni, R. B.: Variations in northern vegetation activity inferred from satellite data of vegetation index during 1981 to 1999, *J. Geophys. Res.-Atmos.*, 106, 20069–20083, doi:10.1029/2000JD000115, 2001. 9122, 9138
- Zhu, Z., Bi, J., Pan, Y., Ganguly, S., Anav, A., Xu, L., Samanta, A., Piao, S., Nemani, R. R., and Myneni, R. B.: Global data sets of vegetation Leaf Area Index (LAI)3g and Fraction of Photosynthetically Active Radiation (FPAR)3g Derived from Global Inventory Modeling and Mapping Studies (GIMMS) Normalized Difference Vegetation Index (NDVI3g) for the period 1981 to 2011, *Remote Sensing*, 5, 927–948, doi:10.3390/rs5020927, 2013. 9126
- 20 Zhuang, Q., McGuire, A. D., O'Neill, K. P., Harden, J. W., Romanovsky, V. E., and Yarie, J.: Modeling soil thermal and carbon dynamics of a fire chronosequence in interior Alaska, *J. Geophys. Res.-Atmos.*, 107, 8147, doi:10.1029/2001JD001244, 2002. 9137
- 25



## Vegetation greening across northern Eurasia

P. Dass et al.

Title Page

Abstract

Introduction

Conclusions

References

Tables

Figures



Back

Close

Full Screen / Esc

Printer-friendly Version

Interactive Discussion



**Table 2.** Validation of GIMMS3g and VIP GPP datasets along with their ensemble mean using flux tower GPP from ten flux tower sites across northern Eurasia. The spatial distribution of the flux tower sites is shown in Fig. 1. Validation was carried out using: (1) Pearson's product moment correlation. It is a measure of the linear dependence between the simulated and observed GPP and it's value ranges from  $-1$  to  $+1$  where  $0$  is no correlation and  $-1/+1$  is total negative or positive correlation; (2) percent bias, which measures the average tendency of the simulated values to be larger or smaller than their observed ones. The optimal value is  $0.0$  with low-magnitude values indicating accurate model simulations. Positive values indicate overestimations and vice versa (Yapo et al., 1996; Sorooshian et al., 1993); (3) Nash–Sutcliffe model efficiency coefficient (Nash and Sutcliffe, 1970). Its values range from  $-\infty$  to  $1$ . An efficiency of  $1$  corresponds to a perfect match of model simulated GPP to the observed data. An efficiency of  $0$  indicates that the model predictions are as accurate as the mean of the observed data, whereas an efficiency less than zero occurs when the observed mean is a better predictor than the model or, in other words, when the residual variance (between modeled and observed values), is larger than the data variance (between observed values and the observed mean). Essentially, the closer the model efficiency is to  $1$ , the more accurate the model is.

Correlation ( <i>R</i> )	GIMMS GPP	VIP GPP	Ensemble mean
Annual	0.71	0.68	0.70
Spring	0.82	0.81	0.81
Summer	0.72	0.64	0.69
Fall	0.64	0.67	0.66
Percent bias	GIMMS GPP	VIP GPP	Ensemble mean
Annual	−16.9%	−19.7%	−18.3%
Spring	−9.1%	−17.3%	−13.2%
Summer	1.9%	−2.1%	−0.1%
Fall	−35.1%	−28.3%	−31.7%
Nash–Sutcliffe Efficiency	GIMMS GPP	VIP GPP	Ensemble mean
Annual	0.36	0.29	0.33
Spring	0.64	0.57	0.61
Summer	0.46	0.40	0.44
Fall	0.13	0.27	0.21



## Vegetation greening across northern Eurasia

P. Dass et al.

[Title Page](#)

[Abstract](#)

[Introduction](#)

[Conclusions](#)

[References](#)

[Tables](#)

[Figures](#)



[Back](#)

[Close](#)

[Full Screen / Esc](#)

[Printer-friendly Version](#)

[Interactive Discussion](#)



**Table 4.** Medians of the distributions of the relative contribution ( $R^2$ ) of each environmental variable of each season to the inter-annual variability in annual GPP (mean of the two datasets). The  $R^2$  values (explained variances) have been calculated after de-trending both the GPP as well as the environmental variable datasets. In each case the total contribution may not add up to 100 %. In these cases the factors behind the unexplained attribution are not identified.

Environmental variable	Annual	Spring	Summer	Autumn
Temperature	11.8 %	7.3 %	33.3 %	2.4 %
Precipitation	5.9 %	2.8 %	7.9 %	2.2 %
Cloudiness	5.3 %	2.5 %	10.5 %	2.5 %
Burnt Area	4.8 %	5.3 %	4.8 %	5.3 %



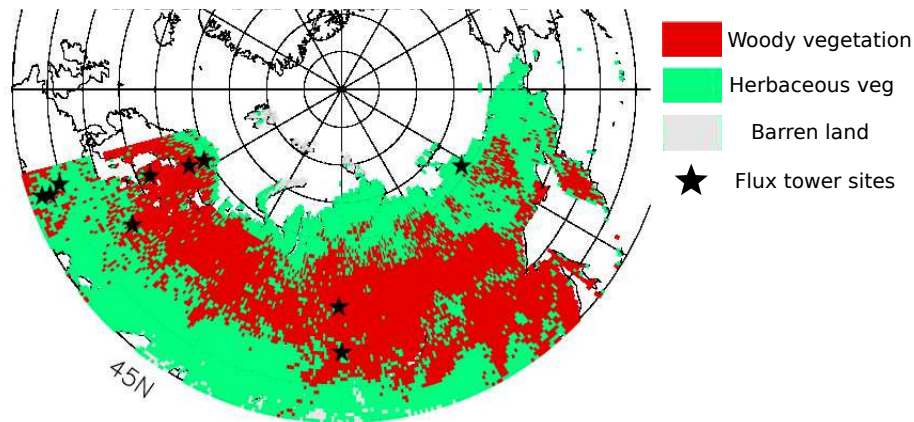


**Figure 1.** Simplified land cover for northern Eurasia for year 2007 overlaid with the spatial distribution of the ten flux tower sites whose GPP (Gross Primary Productivity) data was used to validate the GPP data derived from satellite NDVI (Normalized Difference Vegetation Index). For our statistical analysis, we show the distribution of two fundamental types of vegetation types: (i) herbaceous, i.e. without woody stems, which includes the tundra in the north and the comparatively drier grasslands (the Eurasian Steppe) to the south and (ii) woody vegetation, i.e. plants with woody stems, which includes the boreal forests which appear in the middle and extend from the western to the eastern boundary. This land cover map has been derived from the Moderate Resolution Imaging Spectroradiometer (MODIS) MCD12Q1 Land Cover Product Type 5 Land Cover Product. The map product involve a supervised classification methodology that exploited a global database of training sites interpreted from high-resolution imagery in association with ancillary data (Friedl et al., 2002). The details of the flux tower sites are listed in Table 1. It is apparent that most of the flux tower sites are concentrated towards eastern Europe, i.e. the western margin of the study area. This implies that there is a comparatively limited validation of the GPP of central and eastern part of the study area.

**Vegetation greening across northern Eurasia**

P. Dass et al.

[Title Page](#)

[Abstract](#) | [Introduction](#)

[Conclusions](#) | [References](#)

[Tables](#) | [Figures](#)

[◀](#) | [▶](#)

[◀](#) | [▶](#)

[Back](#) | [Close](#)

[Full Screen / Esc](#)

[Printer-friendly Version](#)

[Interactive Discussion](#)



Vegetation greening  
across northern  
Eurasia

P. Dass et al.

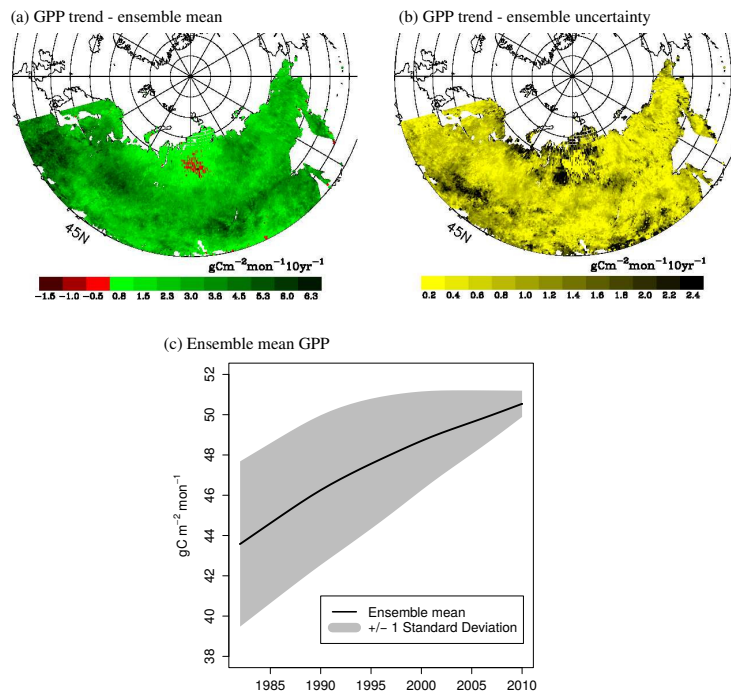


**Figure 2.** Change in annual Gross Primary Productivity (GPP) over the period 1982–2010. **(a)** shows the spatial distribution of trend in GPP as an ensemble mean of the GIMMS3g and VIP GPP datasets. **(b)** shows the spatial distribution of the ensemble uncertainty. The trends have been derived from a linear least squares fit to the GPP time series for GIMMS3g and VIP datasets. Trend values represent the rate of change of productivity per decade ( $\text{gC(Carbon) m}^{-2} \text{month}^{-1} 10 \text{ yr}^{-1}$ ). **(c)** shows yearly change in the GPP (ensemble mean). The black line represents the ensemble mean while the grey area represents the uncertainty (as  $\pm 1$  standard deviation) due to the two datasets having different GPP (spatial mean). The inter-annual variation is smoothed using a smoothing spline (Coefficient = 0.8).

Title Page

Abstract

Introduction

Conclusions

References

Tables

Figures



Back

Close

Full Screen / Esc

Printer-friendly Version

Interactive Discussion



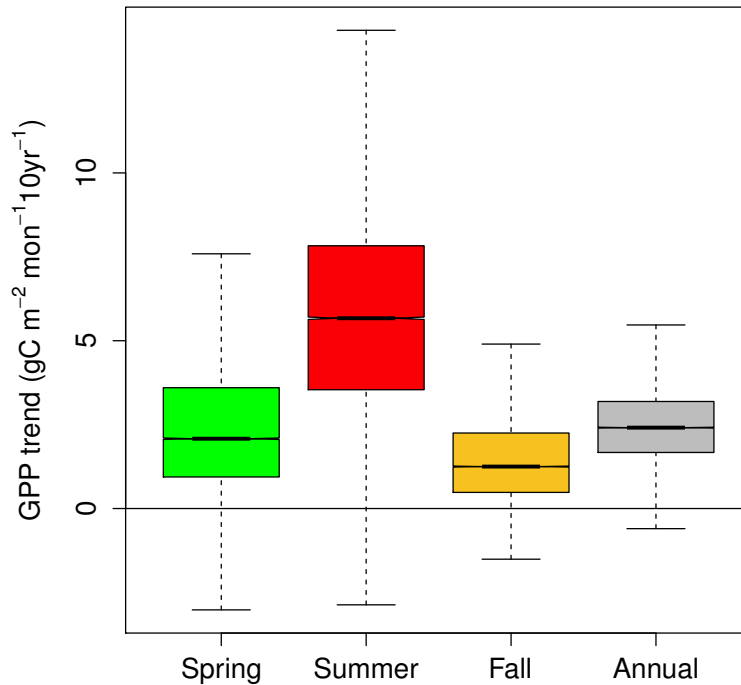


**Figure 3.** Box plot showing grid distributions of seasonal GPP trends for the mean of the GIMMS3g and VIP datasets. The GPP trends are expressed in  $\text{g C m}^{-2} \text{ month}^{-1} 10 \text{ yr}^{-1}$ . The black band and middle notch represent the 2nd quartile or median, box extents mark the 25th (1st quartile) and 75th (3rd quartile) percentiles. Whiskers extend from the smallest non-outlier value to the largest non-outlier value. The colors, green, red, orange and gray represent spring, summer, autumn and annual seasonal trends respectively. As described in Sect. 2.1.2, GPP trends for winter have not been assessed in this study. The presence of all the boxes above the zero line implies a predominantly positive GPP trend from all parts of the growing season.

**Vegetation greening across northern Eurasia**

P. Dass et al.

[Title Page](#)

[Abstract](#) | [Introduction](#)

[Conclusions](#) | [References](#)

[Tables](#) | [Figures](#)

[◀](#) | [▶](#)

[◀](#) | [▶](#)

[Back](#) | [Close](#)

[Full Screen / Esc](#)

[Printer-friendly Version](#)

[Interactive Discussion](#)



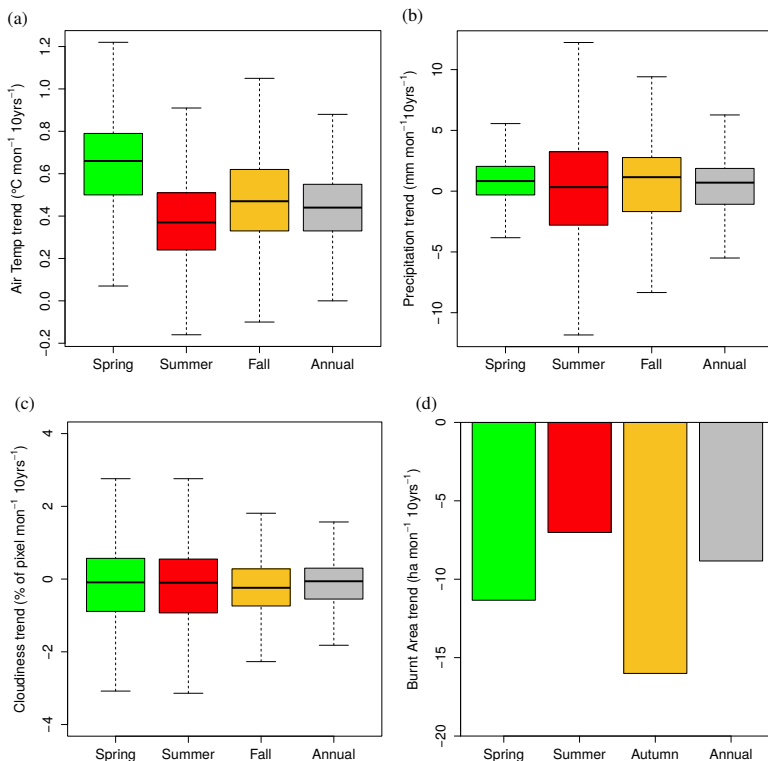


**Figure 4.** Change in the environmental variables over the period of study represented by seasonal trends. **(a–c)** show distribution of 2 m air temperature, precipitation and cloud cover respectively for the period 1982–2008, **(d)** illustrates seasonal trends of total burnt area for the period 1997–2011. The temperature and precipitation data are drawn from the University of Delaware (UDel) dataset (Matsuura and Willmott, 2009). Cloud cover data are taken from the Climatic Research Unit (CRU) dataset (Harris et al., 2014). Burnt area data from the Global Fire Emissions Database (GFED) (Giglio et al., 2010).

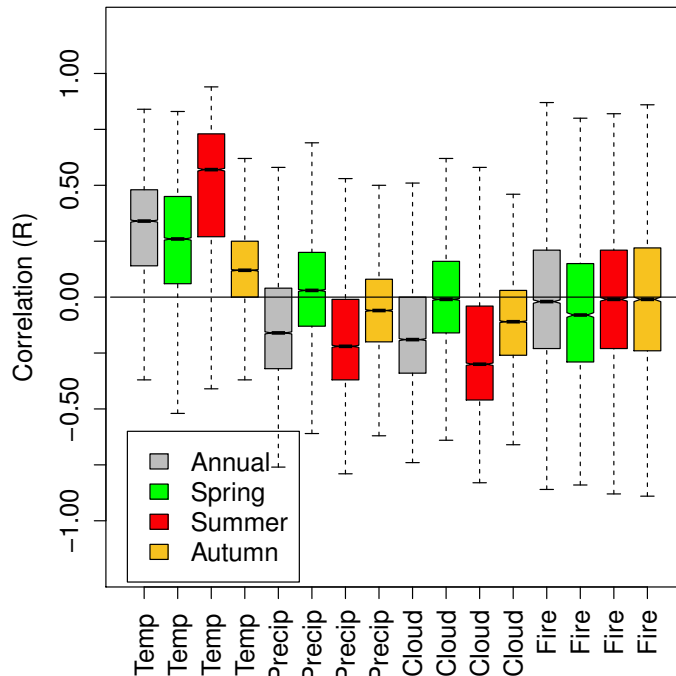


**Figure 5.** Box plots of the distribution for correlation between the satellite derived annual GPP (mean of the two datasets) and the values of each environmental variable for each season after de-trending both sets of values. It is evident that for 3 out of the 4 variables the magnitude of the correlation is highest in summer and among the four variables, only temperature has a strong positive correlation. The values shown are the Pearson's correlation coefficients which are based on the linear least squares trend fit. Correlation values range from  $-1$  to  $+1$ . The location of the box of the box plots on either side of the zero line is a simplified and clear indication of the nature of the correlation between GPP and the variable. Values closer to  $-1$  or  $+1$  indicates strong correlation while those closer to  $0$  indicates weak correlation.

[Title Page](#)

[Abstract](#)

[Introduction](#)

[Conclusions](#)

[References](#)

[Tables](#)

[Figures](#)



[Back](#)

[Close](#)

[Full Screen / Esc](#)

[Printer-friendly Version](#)

[Interactive Discussion](#)



## Vegetation greening across northern Eurasia

P. Dass et al.

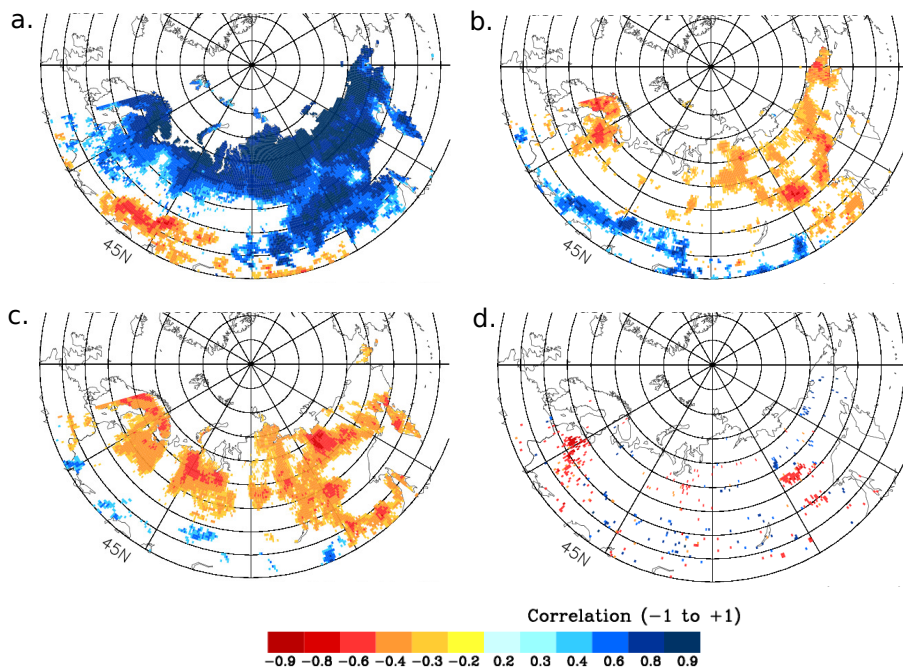


**Figure 6.** Maps showing area characterized by statistically significant (95 % significance level) correlation between de-trended annual GPP (satellite derived and mean of two datasets) and de-trended summer values of each environmental variable. Sub-figures show the correlation between GPP and (a) temperature, (b) precipitation, (c) cloud cover and (d) burnt area. Negative correlations shown with shades of red and positive shown in shades of blue.

Title Page

Abstract

Introduction

Conclusions

References

Tables

Figures

◀

▶

◀

▶

Back

Close

Full Screen / Esc

Printer-friendly Version

Interactive Discussion



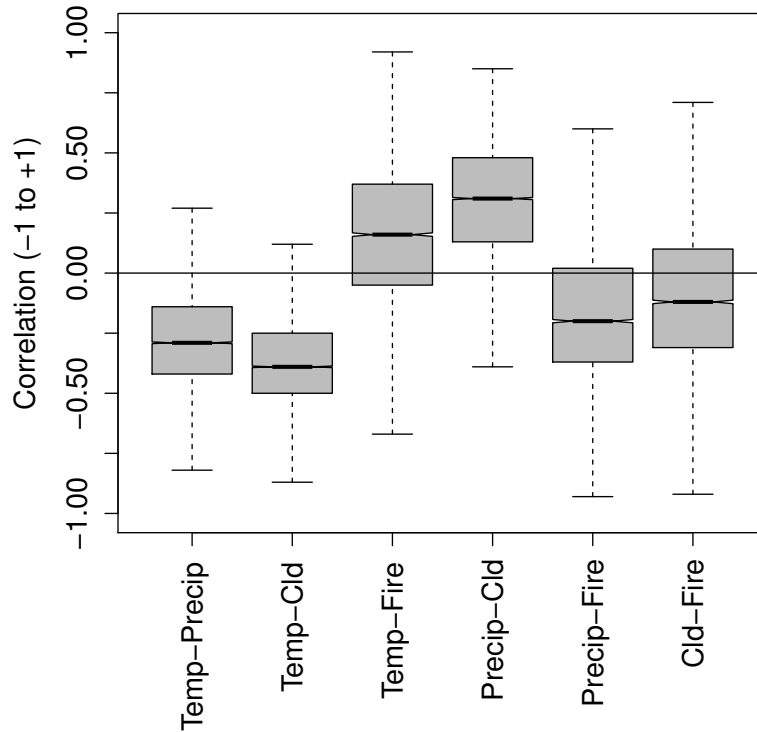


**Figure 7.** Box plots of the distribution for correlation between de-trended values of each environmental variable. The location of the box and in particular the median on the y axis, on either side of the zero line reveals the predominant sign of the correlation.

Title Page

Abstract

Introduction

Conclusions

References

Tables

Figures



Back

Close

Full Screen / Esc

Printer-friendly Version

Interactive Discussion

